Design of a Channel Diplexer for Millimeter-Wave Applications

CHUNG-LI REN

Abstract—The design of millimeter-wave filters is, in principle, no different from the design of conventional waveguide filters. In practice, however, several factors impose limitations on the choice of the filter structure. As a result, new filter structures must be used requiring new synthesis techniques for their design. In this paper, a new channel diplexer structure is described and a synthesis technique for its design is given. The expected electrical performance of the filter, designed using the proposed technique, is verified by measuring the performance of a scaled filter model centered at 3.95 GHz. The results of these measurements are given. The design procedure is also applicable to other waveguide filter structures.

I. Introduction

WAVEGUIDE filters are commonly used in microwave radio systems, since waveguide cavities have much higher intrinsic Q than, for example, TEM line structures. But the intrinsic Q decreases as the frequency increases. Thus even waveguide filters of conventional structure can no longer meet the loss requirements of a millimeter-wave transmission system [1], [2]. Indeed, one of the controlling design objectives for a millimeter-wave channel diplexer is that the intrinsic losses must be kept low for both the through channels and the dropped channel (or the channel to be combined). To fulfill this requirement one might consider the utilization of low-loss modes, oversized waveguides, and cavities [3]–[6]. Consequently, there will be stringent design limitations for the waveguide and cavities of the filter structure, because, within the specified frequency band, no spurious modes should pass through cutoff in the main waveguide and spurious resonant modes in the cavities must be avoided. Furthermore, in order to avoid moding problems, severe limitations also exist in choosing the shapes and the locations of the coupling apertures between the waveguide and the cavities, and of the tuning devices in the intended filter design. In addition, there are physical limitations to the filter design at millimeter-wave frequencies because of the extremely small size. The feasibility of filter fabrication must be considered.

In this paper, a new channel diplexer (Fig. 1) is described that will achieve the various design objectives enumerated in the preceding. The incoming signals in the main waveguide are in the low-loss semicircular $H_{01}^{\circlearrowleft}$ mode and the dropped channel at the output port is restricted to the dominant rectangular waveguide mode. Therefore, unlike conventional waveguide filters with only the dominant mode function involved, the proposed channel diplexer involves more than one mode. Consequently, the circuit elements of its equivalent circuit are functions of the guide wavelengths of different modes, which vary differently with frequency. Therefore, the simple frequency transformation commonly used in waveguide filter synthesis is no longer applicable. A new synthesis technique has been developed for the design of the proposed channel diplexer. The proposed technique is also applicable to other filter structures. The synthesis technique, when used in the diplexer design, provides precise 3-dB bandwidth and high return loss at the common port.

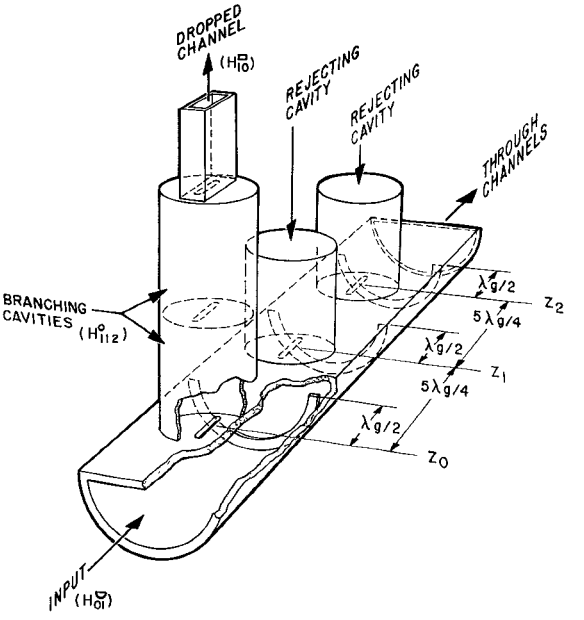

Fig. 1. H_{112}° channel diplexer.

An experimental model of the two-pole channel diplexer of Fig. 1 with a center frequency at 3.95 GHz, a 3-dB bandwidth of 20 MHz, and 0.175 in thick irises, was designed and fabricated. At this frequency the dimensional tolerances of a fabricated filter can be controlled effectively and the design theory can be verified with a high degree of accuracy. The experimental filter

Manuscript received May 30, 1972; revised August 16, 1972. This paper was presented at the 1972 International Microwave Symposium, Chicago, Ill., May 22–24, 1972.

The author is with Bell Telephone Laboratories, Inc., North Andover, Mass. 01845.

with a center frequency at 3.95 GHz is obtained by frequency scaling from a diplexer design intended for 102.76 GHz. Very good agreement has been achieved among design objectives, theoretical performance, and measured performance. Thus it is shown that a channel diplexer involving oversized waveguides, envisioned for use in a millimeter-wave waveguide transmission system, can be designed using the proposed synthesis and design technique.

II. The Channel Diplexer

A two-pole channel diplexer is shown in Fig. 1. A semicircular waveguide propagating the $H_{01}^{\cup}$ mode is chosen as the main guide because of the advantages in loss and bandwidth. Since numerous channel diplexers will be connected in tandem in the repeater station, minimization of the through channel loss is essential. An oversized semicircular waveguide propagating the $H_{01}^{\cup}$ mode provides roughly a three-to-one reduction in loss in comparison with a dominant mode rectangular guide. Furthermore, in the oversized main waveguide of a channel diplexer, spurious modes may be excited. Within the frequency band of interest, the diameter of the main waveguide must be determined so that no mode passes through cutoff, lest it create serious problems in the channel multiplexing system. The semicircular waveguide can provide such a frequency band with 18-percent bandwidth located between the cutoff frequencies of the $H_{12}^{\cup}$ and $E_{31}^{\cup}$ modes. Eighteen percent is considered remarkably wide for an oversized waveguide.

The signals coming from the circular transmission waveguides are in the circular electric H_{01}° mode. A simple waveguide transition from a circular waveguide to a semicircular waveguide can be readily designed by gradually tapering a radial vane into a semicircular metallic sector in the circular waveguide [1].

Narrow rectangular apertures along the center axis of the plane of bifurcation provide convenient and practical couplings between the main waveguide and the resonant cavities [5], [6]. The excitation of spurious modes can be made negligible for sufficiently narrow apertures that will respond mainly to the $H_{01}^{\cup}$ mode ($H_{02}^{\cup}$ mode is below cutoff).

Circular cavities[1] are used in the design with H_{11N}° being the resonant mode. N represents the cavity length in terms of the number of half wavelengths of the H_{11}° mode. For larger mode index N, the intrinsic loss of the cavity becomes lower. However, larger N also means narrower bandwidth for the cavity to be free of spurious resonance modes. In the proposed structure, H_{112}° modes are used. The circular cavities used in the design are oversized with both H_{11}° and E_{01}° modes above cutoff. Typically, over 13-percent bandwidth can be provided by such oversized H_{112}° cavities with the band located between the resonant frequencies of the spurious E_{011}° and E_{012}° modes. Over 15-percent bandwidth can be provided by the H_{111}° cavity having the same radius. If the cavities are not oversized, i.e., if the cavities propagate only the dominant mode, still broader bandwidth is obtainable.

As in conventional waveguide filter structures, the aperture coupled H_{112}° cavities have asymmetrical frequency responses [7]. They are compensated to be symmetrical by the semicircular ridges in the main waveguide (Fig. 1). These ridges do not disturb the circular symmetry of the electromagnetic fields of the $H_{01}^{\cup}$ mode and, therefore, excite no spurious modes. Furthermore, in order that the compensating ridges compensate for the asymmetry of the cavity frequency response without significantly affecting the aperture coupling, they are placed $\lambda g/2$ away from the coupling aperture locations.

III. Synthesis—Network Representation of the Channel Diplexer as a Two-Pole Complementary Filter

Since the shapes and locations of the coupling apertures and tuning devices are carefully chosen as explained in the preceding section, only the $H_{01}^{\cup}$ mode in the semicircular guide and the H_{11}° mode in the circular cavities are assumed propagating. All other propagating modes are not excited by the coupling apertures and tuning devices. The longitudinal magnetic field of the $H_{01}^{\cup}$ mode in the semicircular guide is coupled to the transverse magnetic fields of the H_{112}° mode in the cavities through the narrow rectangular apertures. The two bandpass cavities are coupled by the transverse magnetic fields of the H_{112}° modes in each of the two cavities through a narrow rectangular aperture. The dropped channel is coupled to the transverse magnetic fields of the $H_{10}^{=}$ mode in the rectangular guide.

The design of the channel diplexer requires the availability of known transmission and reflection properties of the coupling apertures and tuning devices in the filter structure, from which an equivalent circuit can be derived. The latter is required in the filter synthesis. The theoretical solution of the filter structure is obtained from small aperture and small obstacle theory [8], [9]. The equivalent circuit of the channel diplexer is subsequently derived [10], [11] as shown in Fig. 2. For convenience in presentation, the equivalent circuits of the semicircular ridges are not included in Fig. 2, but will be introduced later on to show that without their presence in the filter structure in Fig. 1, the equivalent circuit as shown in Fig. 2 will not be a complementary filter [12].

Fig. 5 shows the network transforming steps for

[1] The cross section of the resonant cavities may also be either rectangular or elliptical. The circular cavities have higher intrinsic Q than the rectangular cavities (U. S. Patent 3 668 564).

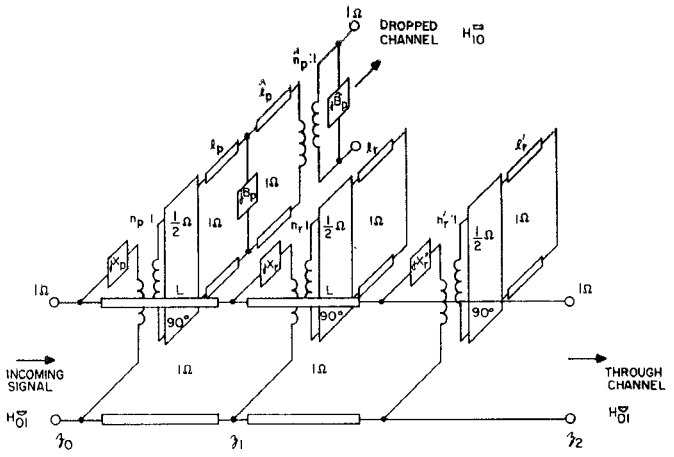

$$X_p=-\frac{1}{2A} \qquad B_p=-\frac{(x_{11}^2-1)J_1^2(x_{11})}{x_{11}^2}\frac{\bar{a}_1^2}{M_{xx}}\lambda g_{11}$$

$$\hat{B}_p=-\frac{ab}{4\pi M_x}\lambda g_{10} \qquad n_p=(B/A)^{\frac{1}{2}}$$

$$\hat{B}_p=\left(\frac{\lambda g_{10}}{\lambda g_{11}}\right)\frac{x_{11}^2}{(x_{11}^2-1)J_1^2(x_{11})}\frac{ab}{\bar{a}_1^2}$$

$$A=\frac{x_{01}^2}{2\pi^2 J_0^2(x_{01})}\frac{M_1}{a_1^4}\lambda g_{01} \qquad B=\frac{2x_{11}^2}{(x_{11}^2-1)J_1^2(x_{11})}\frac{M_1}{\bar{a}_1^2}\frac{1}{\lambda g_{11}}$$

$$X_r=-\frac{1}{2A_r} \qquad X_r'=-\frac{1}{2A_r'} \qquad n_r=(B_r/A_r)^{-1} \qquad n_r'=(B_r'/A_r')^{-1}$$

$$A_r=\frac{x_{01}^2}{2\pi^2 J_0^2(x_{01})}\frac{M_2^4}{a_1^4}\lambda g_{01} \qquad B_r=\frac{2x_{11}^2}{(x_{11}^2-1)J_1^2(x_{11})}\frac{M_2}{a_1^2}\frac{1}{\lambda g_{11}}$$

$$A_r'=\frac{x_{01}^2}{2\pi^2 J_0^2(x_{01})}\frac{M_2^4}{a_1^4}\lambda g_{01} \qquad B_r'=\frac{2x_{11}^2}{(x_{11}^2-1)J_1^2(x_{11})}\frac{M_2}{a_1^2}\frac{1}{\lambda g_{11}}$$

λg_{01}=wavelength of H_{01}° mode
λg_{11}=wavelength of H_{11}° mode
λg_{10}=wavelength of $H_{10}^{\square}$ mode
a=broad side of rectangular guide
b=narrow side of rectangular guide
a_1=radius of semicircular guide
$\bar{a}_1$=radius of circular cavity
M_1=magnetic polarizability of the aperture at z_0
M_2=magnetic polarizability of the aperture at z_1
M_3=magnetic polarizability of the aperture at z_2
M_x=magnetic polarizability of the aperture at x_0
M_{xx}=magnetic polarizability of the aperture between two bandpass cavities

Fig. 2. Equivalent circuit derived from small aperture theory.

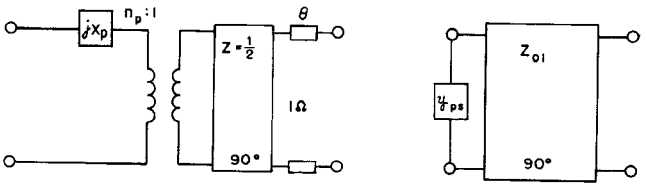

$$Z_{01}=\left[\frac{1+(B/2)^2}{AB}\right]^{\frac{1}{2}} \qquad y_{ps}=j2A\frac{2+(B/2)^2}{1+(B/2)^2} \qquad \theta=\tan^{-1}\left(\frac{2}{B}\right)$$

Fig. 3. Network transformation.

obtaining the prototype circuit of the bandpass section [Fig. 5(c)]. Applying the network transformations of Fig. 3 and Fig. 4 to the equivalent circuit in Fig. 5(a), a typical bandpass filter circuit is obtained as portrayed in Fig. 5(b).[2] Thus a prototype bandpass circuit can be derived from Fig. 5(b) consisting of a series element Z_p

[2] l in Fig. 5(a) is half wavelength or a number (integers) of half wavelengths depending upon the design specifications.

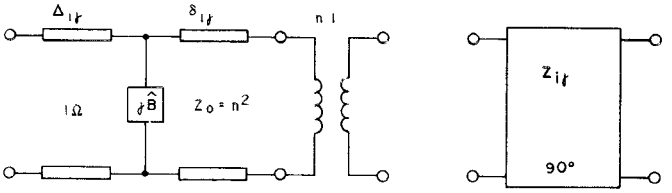

$$Z_{1f}=(\tan\delta_{1f}\tan\Delta_{1f})^{\frac{1}{2}} \qquad \hat{B}=\frac{\cos^2\Delta_{1f}-\sin^2\delta_{1f}}{\sin\Delta_{1f}\cos\Delta_{1f}} \qquad n^2=\frac{\sin\Delta_{1f}\cos\Delta_{1f}}{\sin\delta_{1f}\cos\delta_{1f}}$$

Fig. 4. Network transformation.

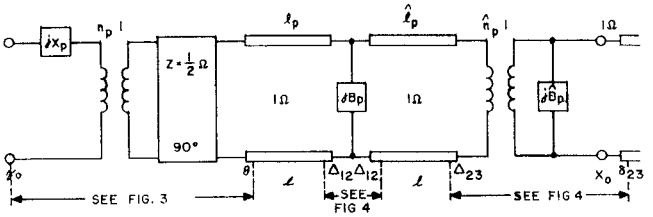

(a)

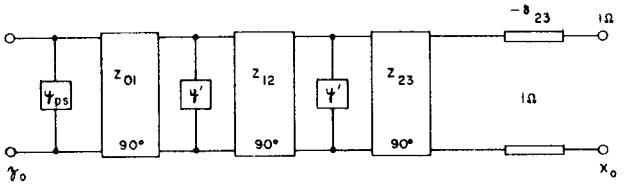

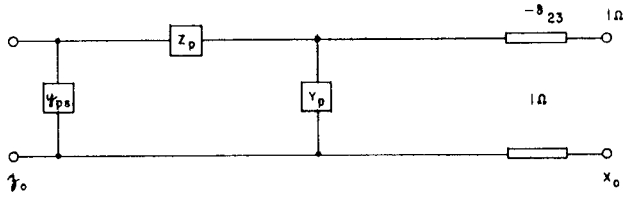

(b)

$$Y_{ps}=j2A\frac{2+(\frac{B}{2})^2}{1+(\frac{B}{2})^2} \qquad y'=-j\sin\beta_{11}\ell$$

$$Z_p=-jZ_{01}^2\sin\beta_{11}\ell \qquad \ell=t_p-\Delta_{12}-\theta=\hat{\ell}_p-\Delta_{12}-\Delta_{23}$$

$$Y_p=-j\left(\frac{Z_{12}}{Z_{01}}\right)^2\sin\beta_{11}\ell \qquad \theta=\tan^{-1}\left(\frac{2}{B}\right)$$

$$Z_{01}=\left[\frac{1+(B/2)^2}{AB}\right]^{\frac{1}{2}} \qquad \Delta_{12}=\tan^{-1}\frac{-B_p+\sqrt{4+B_p^2}}{2}$$

$$Z_{12}=(-B_p+\sqrt{4+B_p^2})/2 \qquad \Delta_{23}=\frac{1}{2}\tan^{-1}\frac{2\hat{B}_p\hat{n}_p^2}{1+\hat{B}_p^2-\hat{n}_p^4}+\frac{\pi}{2}$$

$$Z_{23}^2=(Z_{12}/Z_{01})^2 \qquad \delta_{23}=\tan^{-1}\{\hat{n}_p^2\cot\Delta_{23}-\hat{B}_p\}$$

$$=\hat{n}_p-\hat{B}_p\tan\left\{\frac{1}{2}\tan^{-1}\frac{\hat{B}_p\hat{n}_p^2}{1+\hat{B}_p^2-\hat{n}_p^4}\right\}$$

(c)

Fig. 5. Network transformation for bandpass section.

and a shunt element Y_p [Fig. 5(c)]. Z_p and Y_p are shown analytically in the vicinity of the center frequency of the channel diplexer f_0 as

$$\left.\begin{matrix} Z_p(f) \\ Y_p(f) \end{matrix}\right\} \propto \beta_{01}(f) \frac{\beta_{11}(f) - \beta_{11}(f_0)}{\beta_{11}(f)\beta_{11}(f_0)} . \tag{1}$$

β_{01} and β_{11} are the phase velocities of the $H_{01}^{\circlearrowleft}$ and H_{11}° modes, respectively. It is also shown in the network transformation that, in order to obtain Z_p and Y_p as shown in (1), a 1-Ω negative line length $-\delta_{23}$ must be added at x_0 and that a shunt reactance y_{ps} must be extracted at z_0. The negative line length represents merely a phase shift of the rectangular waveguide port at x_0, while the shunt reactance y_{ps} must be compensated (removed from the circuit at z_0). It is to be shown that y_{ps} can be compensated by a semicircular ridge as portrayed in Fig. 1.

y_{ps} of Fig. 5 may be written in approximation as ($B^2 \ll 1$ in a practical design)

$$y_{ps} \simeq j \frac{2\chi_{01}^2}{\pi^2 J_0^2(\chi_{01})} \frac{M_1}{a_1^4} \lambda g_{01}. \tag{2}$$

It can be shown from small obstacle theory that the equivalent circuit of a thin semicircular ridge is a positive shunt reactance identical to y_{ps} as a function of frequency but opposite in sign.

$$y_{pd} = -j \frac{\chi_{01}^2}{\pi^2 J_0^2(\chi_{01})} \frac{M}{a_1^4} \lambda g_{01}. \tag{3}$$

M is the magnetic polarizability of the ridge that perturbs the longitudinal magnetic field of the $H_{01}^{\circlearrowleft}$ mode perpendicular to the surface of the ridge. For the time being, let us assume that the semicircular ridge is placed at z_0 instead of $\lambda g/2$ away from z_0 as shown in Fig. 1. Thus it becomes clear from (2) and (3) that y_{ps} can be compensated [removed from the circuit as portrayed by the dotted lines in Fig. 6(a)] by the semicircular ridge for all frequencies.

A similar prototype network representation for the bandstop section can be obtained from the following network transformations. Each coupling waveguide as represented by a line length L in Fig. 6(a) is replaced by the familiar equivalent circuit shown in Fig. 7. The reactance elements y as well as the characteristic impedance of the impedance inverters Z_0 are functions of frequency. It should be noted that the characteristic impedance of the impedance inverter is normalized to unity at the design center frequency of the channel diplexer but deviates significantly from unity at the 3-dB points of the filter, even for very narrow-band designs. To achieve good design accuracy, the exact frequency function of this characteristic impedance is used in the synthesis instead of unity as conventionally assumed. Applying the network transformation of Fig. 7 to the two coupling waveguides in Fig. 6(a) and after the subsequent cancellation of the two impedance inverters, the equivalent circuit in Fig. 6(a) is transformed into its alternate representation in Fig. 6(b). The series impedance is

$$Z_s = Z_0^2(y_s + 2y) \tag{4}$$

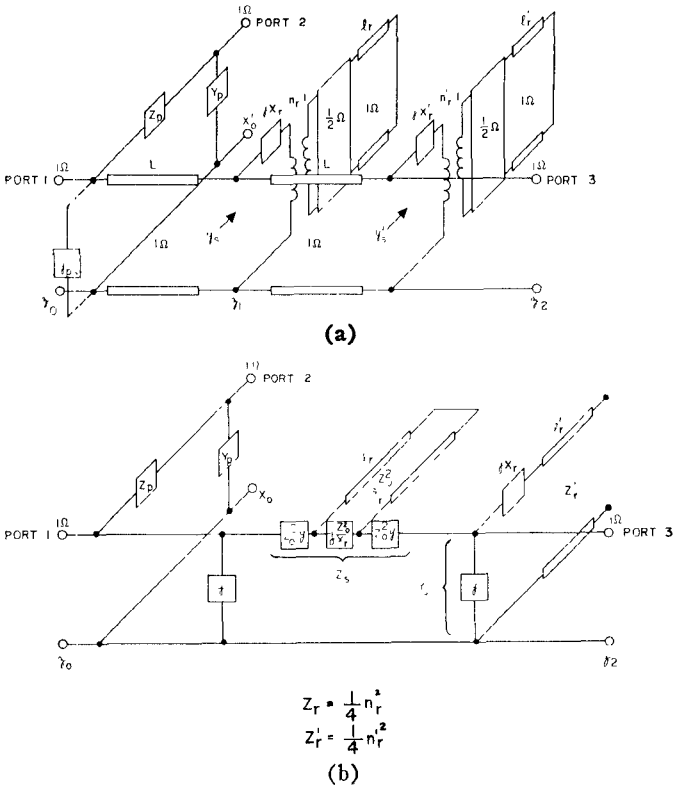

Fig. 6. Equivalent circuit of the uncompensated channel diplexer.

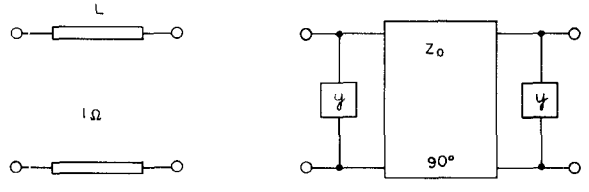

$$Z_0 = \sin\beta_{01}L$$
$$\psi = -j \cot\beta_{01}L$$

Fig. 7. Network transformation.

and the shunt admittance is

$$Y_s = y_s' + y. \tag{5}$$

Where y_s and y_s' are the shunt input admittances at z_1 and z_2, respectively [Fig. 6(a)],

$$y_s = \frac{j2A_r}{1 + \frac{B_r}{2}\cot\beta_{11}l_r} \tag{6a}$$

and

$$y_s' = \frac{j2A_r'}{1 + \frac{B_r'}{2}\cot\beta_{11}l_r'} . \tag{6b}$$

If the shunt admittance y at z_0 is neglected, it can be shown that for Fig. 6(b) to be a complementary filter

(i.e., the input admittance at the common port (port 1) is frequency invariant (1 Ω) when port 2 and port 3 are terminated into a 1-Ω load), the following conditions must be satisfied for all frequencies:

$$Z(f) = Z_p(f) = \frac{1}{Y_s(f)} \tag{7}$$

$$Y(f) = Y_p(f) = \frac{1}{Z_s(f)} \tag{8}$$

and

$$Z(f) = 2Y(f). \tag{9}$$

Consequently, the scattering coefficients are

$$|S_{11}| = 0 \tag{10a}$$

$$|S_{12}|^2 = \frac{1}{1 + |Z(f)Y(f)|^2} \tag{10b}$$

$$|S_{13}|^2 = \frac{|Z(f)Y(f)|^2}{1 + |Z(f)Y(f)|^2} \tag{10c}$$

$$|S_{22}|^2 = \left[\frac{|Z(f)Y(f)|^2}{1 + |Z(f)Y(f)|^2}\right]^2 \tag{10d}$$

$$|S_{33}|^2 = \left[\frac{1}{1 + |Z(f)Y(f)|^2}\right]^2 \tag{10e}$$

$$|S_{23}|^2 = |S_{32}|^2 = \frac{|Z(f)Y(f)|^2}{[1 + |Z(f)Y(f)|^2]^2}. \tag{10f}$$

The condition specified by (9) is fulfilled as it is evidently shown in (1). To fulfill the conditions specified by (7) and (8), it is imperative that Y_s in (5) and Z_s in (4) are inverse functions of Z_p and Y_p, respectively. Z_0^2 in (4) is an even function of frequency centered at f_0. y in (4) and (5) are odd functions of frequency similar to (1) but with negligible magnitudes. Thus Z_s and Y_s of (4) and (5) will be approximately inverse functions of Z_p and Y_p as in (1) if y_s and y_s' are inverse functions of (1). However, y_s and y_s' in (6) do not have such frequency responses. y_s can be shown analytically in the vicinity of f_0 as

$$y_s \propto \frac{1}{\beta_{01}(f)} \frac{\beta_{11}(f_0)}{\beta_{11}(f) - \beta_{11}(f_0)} \tan \beta_{11}(f) l_r. \tag{11}$$

Similarly, y_s' can also be shown as in (11). The inverse of (11) is different from (1) by a factor of $\beta_{11}(f) \cot \beta_{11}(f) l_r$. Z_s and Y_s of Fig. 6(b) do not satisfy (7) and (8), and, therefore, the equivalent circuit in Fig. 6 is not a complementary filter.

From (11) and (1), one can easily see that by multiplying (6) with $K\beta_{11}(f) \cot \beta_{11}(f) l_r$, a modified shunt input admittance at either z_1 or z_2 can be created as an

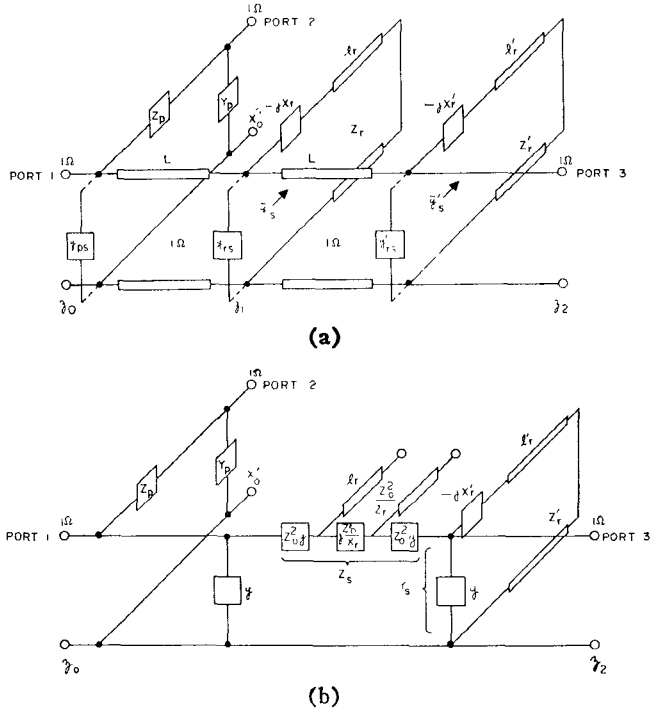

Fig. 8. Equivalent circuit of the channel diplexer as a complementary filter.

inverse function of (1). K of the multiplier, $K\beta_{11}(f) \cot \beta_{11}(f) l_r$, is a constant that must be properly chosen such that the multiplication of (6) by the multiplier will be physically realizable in the network. An appropriate multiplier is found to be $-(B_r/2) \cot \beta_{11}(f) l_r$, where $B_r \propto \beta_{11}(f)$. Let $\bar{y}_s$ and $\bar{y}_s'$ be the modified shunt input admittance at z_1 and z_2. We then have

$$\bar{y}_s = y_s\left(-\frac{B_r}{2} \cot \beta_{11}(f) l_r\right) = y_s - j2A_r \tag{12}$$

and

$$\bar{y}_s' = y_s'\left(-\frac{B_r'}{2} \cot \beta_{11}(f) l_r'\right) = y_s' - j2A_r'. \tag{13}$$

Equations (12) and (13) signify the extraction of shunt negative reactances $y_{rs} = j2A_r$ and $y_{rs}' = j2A_r'$ at z_1 and z_2 [Fig. 8(a)], respectively. $\bar{y}_s^{-1}$ and $\bar{y}_s'^{-1}$ are shown in the vicinity of f_0 as

$$\left.\begin{matrix}\bar{y}_s^{-1} \\ \bar{y}_s'^{-1}\end{matrix}\right\} \propto \beta_{01}(f) \frac{\beta_{11}(f)\beta_{11}(f_0)}{\beta_{11}(f) - \beta_{11}(f_0)}. \tag{14}$$

We may now conclude that a complementary filter can be obtained from Fig. 6(a) by extracting y_{rs} at z_1 and y_{rs}' at z_2. y_{rs} and y_{rs}' are identical to y_{pd} of (3) as functions of frequency but opposite in sign. Therefore, y_{rs} and y_{rs}' can be compensated for by the semicircular ridges at z_1 and z_2 for all frequencies [removed from the

circuit as indicated by the dotted lines shown in Fig. 8(a)]. A canonical circuit representation of a two-pole complementary filter is finally obtained as shown in Fig. 8(b), where

$$Z_s = Z_0^2(\bar{y}_s + 2y) \simeq \frac{1}{Y_p} \tag{15}$$

$$Y_s = \bar{y}_s' + y \simeq \frac{1}{Z_p} \tag{16}$$

$$Z_p = 2Y_p. \tag{17}$$

Thus the channel diplexer can be designed by computing the polarizabilities of the coupling apertures and the cavity lengths from the solutions of (10), (15), (16), and (17). To achieve precise 3-dB bandwidth specified in the design, the design parameters are computed at either one of the two half-power points. Let f_c be the half-power frequency. Then

$$|Z_p(f_c)| = \sqrt{2} = \frac{1}{|Y_s(f_c)|} \tag{18}$$

and

$$|Y_p(f_c)| = \frac{1}{\sqrt{2}} = \frac{1}{|Z_s(f_c)|}. \tag{19}$$

The design parameters are computed from (18) and (19). The design accuracy is shown by a typical design of the channel diplexer with a center frequency of 102.76 GHz and a 3-dB bandwidth of 520 MHz. Substituting the design parameters obtained from the design program into the equivalent circuit in Fig. 2(a), the theoretical performance of the channel diplexer is analyzed and shown in Fig. 9. It exhibits precise 3-dB bandwidth, over 40-dB in-band return loss (VSWR <1.02) and over 30-dB out-of-band return loss (VSWR <1.05).

However, the computed theoretical performance in Fig. 9 is based on an assumption made in the preceding synthesis that the negative reactances y_{ps}, y_{rs}, and y_{rs}' are compensated for by the semicircular ridges located at z_0, z_1, and z_2 as in Fig. 8(a), i.e., directly under the coupling apertures in the main waveguide of the channel diplexer. However, the presence of the compensation ridges directly under the coupling apertures will perturb the longitudinal magnetic field of the incident $H_{01}^{\circlearrowleft}$ mode close to the apertures and will alter the aperture couplings computed in the design program. In order that the compensating ridges compensate for the asymmetry of the cavity frequency response without significantly affecting the aperture couplings, they are placed $\lambda g/2$ away from coupling aperture locations (Fig. 1). This will preserve the good in-band performance achieved by the design program while degrading the out-of-band return loss (Fig. 10). A computer optimization program was then used to optimize the out-of-band

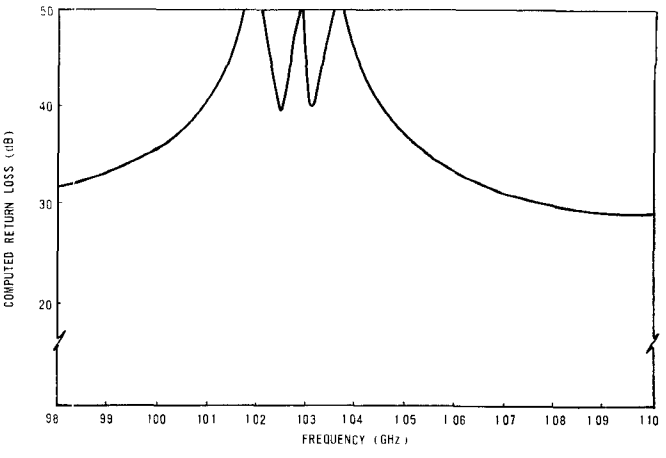

(a)

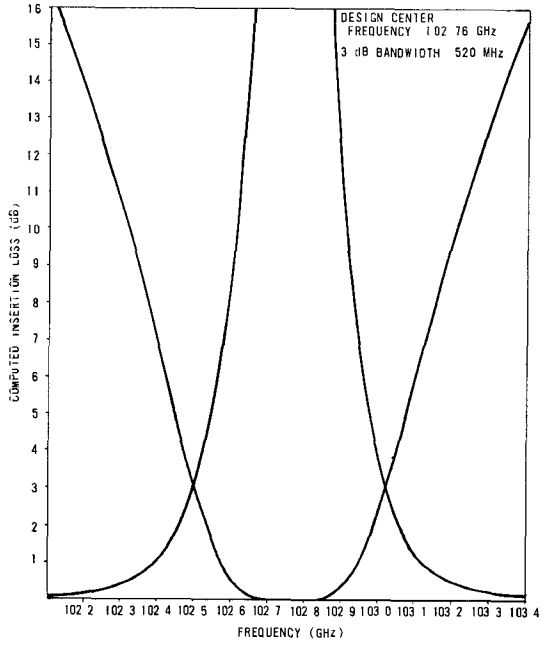

(b)

Fig. 9. (a) Computed return loss of 102.76-GHz channel diplexer design. (b) Computed insertion loss of 102.76-GHz channel diplexer design.

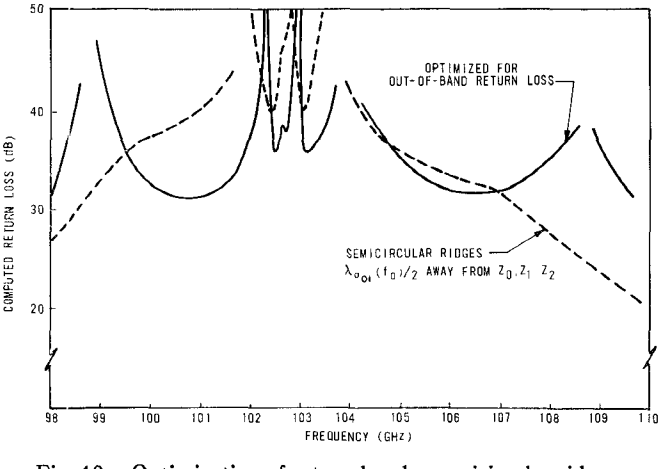

Fig. 10. Optimization of return loss by semicircular ridges.

return loss by varying either the dimensions of the compensating ridges or their locations in the main waveguide relative to the locations of the coupling apertures or both. If the channel diplexer is designed for use in a frequency band less than 13-percent wide, it is found that only the dimensions of the compensating ridges should be varied to achieve better than 1.05 VSWR for the entire band without having to alter other design parameters. The result is shown in Fig. 10. For bandwidth larger than 13 percent a small variation of the locations of the compensating ridges becomes necessary. In some extreme cases of the broad-band design a few percent change of the aperture coupling of the two bandstop cavities are needed. It has also been shown that more than three compensating ridges can be used to achieve better results.

IV. Experimental Design

An experimental model of the channel diplexer of Fig. 1 with center frequency at 3.95 GHz, a 3-dB bandwidth of 20 MHz, and 0.175 in thick irises, was designed and fabricated (Fig. 11). At this frequency the dimensional tolerances of a fabricated filter can be controlled effectively and the design theory can be verified with a high degree of accuracy. This filter is a scaled version of the diplexer design shown in Fig. 9 with a center frequency of 102.76 GHz and a 3-dB bandwidth of 520 MHz.

The equivalent circuit of the channel diplexer used in the design program and synthesis is derived from a first-order solution of electromagnetic scatterings from the coupling apertures. The design program computes the polarizabilities of these apertures. In small aperture theory the aperture dimensions may be computed from these polarizabilities provided that the aperture dimensions are small compared to wavelength and that the apertures are infinitesimally thin. However, in practical designs for millimeter wave applications, the rectangular apertures must be thick for practical purposes. In this experimental design, the apertures of the scaled model at 3.95 GHz are 0.175 in thick and 0.4 in wide. The length of the apertures are either comparable to, or larger than, a quarter wavelength. In order to hold the accuracy to the design specification, the correlation between the computed polarizabilities of the design program and their corresponding aperture lengths, as well as the required length of the coupling waveguides of the bandstop section, is established by measurements.

Fig. 12 shows the measured return loss at the input port of the semicircular waveguide and Fig. 13 shows the measured insertion loss for the through channels as well as the dropped channel. The measured performance compares very well with the theoretical performance in Fig. 9(b) and Fig. 10, based on the corresponding frequency scales as displayed in Fig. 12.

The experimental model was made of machined brass.

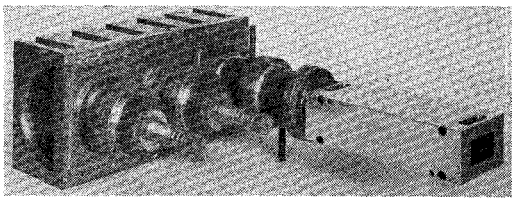

Fig. 11. Experimental channel diplexer.

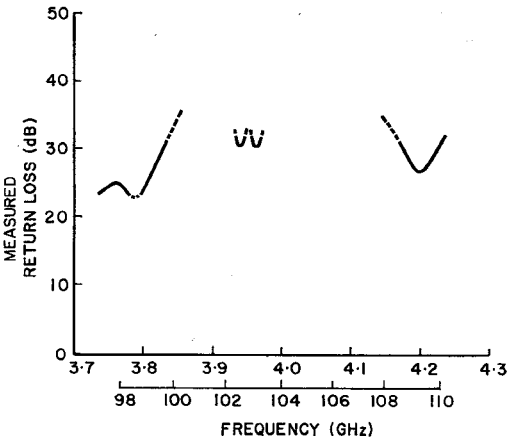

Fig. 12. Measured return loss.

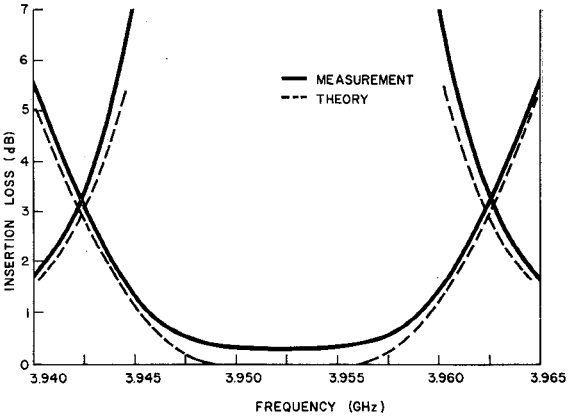

Fig. 13. Measured insertion loss.

The measured loss at the center of the dropped channel is 0.29 dB, as compared to 0.18 dB computed theoretically using dc conductivity. If copper were used, the measured loss would be estimated at about 0.15 dB, as compared to 0.093-dB theoretical loss. This estimate is based on the relative dc conductivities of brass and copper.

V. Summary

It has been shown that a channel diplexer, envisioned for use in a millimeter-wave waveguide transmission system, can be designed. Agreement has been established among design objectives, theoretical performance, and measured performance of a scaled model. When the experimental model is scaled to 102.76 GHz, it should

have a 3-dB bandwidth of 520 MHz and an operating band of over 12 GHz. If the waveguide surface roughness could be scaled, the minimum transmission loss of the dropped channel would be 0.8 dB.[3] However, in practice a surface roughness of 8 μin is expected and the loss is likely to become higher; but it should be less than 1.5 dB.[4] Using the proposed scheme in the channel diplexer design, the channel multiplexing can be accomplished with low loss for both the dropped channel and the through channels. The excellent return loss at the common port over a wide band also permits the connection of numerous channel diplexers in tandem as is required in a waveguide transmission system. The application of the filter at millimeter-wave frequencies requires development of manufacturing techniques.

It has also been shown that the synthesis method developed in this paper will enable the designer to achieve excellent design accuracy for filter structures involving more than one mode. The conventional method using a simple frequency transformation is no longer applicable. Even in the case where the conventional method does apply, the proposed synthesis technique provides better design accuracy because: 1) the bandstop-type cavities are properly compensated; 2) exact network representations of the coupling waveguide between the bandstop-type cavities are used directly in the synthesis; and 3) in the design program the circuit elements are matched at the 3-dB point for fulfilling the complementary condition.

[3] 0.8 dB is estimated from the measured loss of the scaled filter under the assumptions that the loss is proportional to $\sqrt{f}$ and that the filter is made of copper.

[4] This figure is estimated from the measured intrinsic Q of a single cavity at 92 GHz with respect to those measured at 3.95 GHz.

Acknowledgment

The author wishes to thank H. C. Wang for helpful suggestions and discussions in arriving at the basic filter configuration, R. M. Chen for consultations concerning computer optimization program, and F. G. Joyal for his assistance with measurements.

References

[1] S. E. Miller, "Waveguide as a communication medium," *Bell Syst. Tech. J.*, vol. 33, p. 1209, 1954.
[2] W. M. Hubbard *et al.*, "A solid-state regenerative repeater for guided millimeter-wave communication systems," *Bell Syst. Tech. J.*, pp. 1977–2018, Nov. 1967.
[3] E. A. Marcatili, "Channel-dropping filter in the millimeter region using circular electric modes," *IRE Trans. Microwave Theory Tech.*, vol. MTT-9, pp. 176–182, Mar. 1961.
[4] A. L. SaLa and H. M. Barlow, "Channel-dropping filter for millimeter waves in circular waveguide," *Proc. Inst. Elec. Eng.*, June 1969.
[5] S. E. Miller, U. S. Patent 3 112 460, Nov. 26, 1963.
[6] S. Iiguchi *et al.*, "A 48 Gc centre excited type channel branching filter for circular electric waves," *Rev. Elec. Commun. Lab.*, vol. 9, pp. 421–427, 1961.
[7] R. M. Kurzrok, "Trimming improves response of waveguide band-reject filter," *Electron. Des.*, p. 116, Nov 1967.
[8] H. A. Bethe, "Theory of diffraction by small holes," *Phys. Rev.*, vol. 66, p. 163, 1944.
[9] L. B. Felsen and W. K. Kahn, "Network properties of discontinuities in multi-mode circular waveguide," *Proc. Inst. Elec. Eng.*, Feb. 1962.
[10] C. L. Ren, "Implementation of conservation-of-energy condition to small obstacle and small aperture theory," *IEEE Trans Microwave Theory Tech.* (Corresp.), vol. MTT-20, pp. 488–490, July 1972.
[11] ——, "Network representation for lossless symmetrical discontinuities in a multimode waveguide," *IEEE Trans. Microwave Theory Tech.*, vol. MTT-14, pp. 81–85, Feb. 1966.
[12] E. A. Guillemin, *Synthesis of Passive Networks.* New York: Wiley, 1957.